ARTICLE

Predictive Chirality Sensing via Schiff Base Formation

Samantha L. Pilicer,[‡] Michele Mancinelli,[†] Andrea Mazzanti,*[†] Christian Wolf*[‡]

Received 00th January 20xx,
Accepted 00th January 20xx

DOI: 10.1039/x0xx00000x

Among the large number of chiroptical sensors that have been developed to date, few allow rational determination of the absolute configuration of chiral substrates together with quantitative *ee* analysis. We have prepared and tested stereodynamic *N*-aryl aminobenzaldehyde sensors that bind chiral amines via Schiff base formation. The covalent binding of the amine substrate generates a conformational bias in the chromophoric sensor moiety which results in characteristic CD signals. Computational analysis revealed that CD prediction of the sign of the Cotton effect and thus determination of the absolute configuration of the substrate becomes practical with a sterically crowded sensor design because the number of conformations to be considered is largely reduced and the chiroptical sensor response is less sensitive to conformational equilibria. The amplitude of the measured CD signal can be used for quantitative *ee* analysis of nonracemic amine samples with the help of a calibration curve.

Introduction

The introduction of new methods for the stereochemical analysis of chiral compounds is essential to enable progress in asymmetric synthesis, materials sciences and other chemical disciplines. The determination of absolute configuration and enantiomeric excess (*ee*) of chiral amines which play a dominant role in biological processes and drug development initiatives is particularly important and remains a challenging task. In this regard, optical methods using UV, fluorescence and circular dichroism (CD) spectroscopy have become quite popular in recent years.[1] Berova,[2] Kim, Hong and Chin,[3] Anslyn,[4] Anzenbacher,[5] Pu,[6] Borhan,[7] Feng, [8] Wolf[9] and others[10] have developed a variety of optical probes that undergo chiral recognition and amplification processes with amines and derivatives thereof via various covalent binding strategies including Schiff base formation.

Some of the most successful innovations in the realm of chirality sensing have undoubtedly been motivated by an increasing demand for fast optical assays that can exploit parallel screening technology.[11] Accordingly, many probes that bind the target substrate through Schiff base formation have been introduced with the common goal to achieve *ee* analysis for chiral amines with minute analyte quantities. Absolute configuration, however, cannot often be predicted and must instead be determined by comparison of the induced UV, fluorescence or CD signal with the response of the optical sensor to a reference sample. Stereochemical assignments based on such an empirical approach are unreliable when the analysis of new compounds is required or when a reference is unavailable. The possibility to rationally elucidate the absolute configuration of chiral substrates from the induced Cotton effect would extend the use of Schiff base chirality sensors to the stereochemical analysis of new compounds. In the pharmaceutical sciences, for example, this remains a very important goal. We therefore have decided to involve computational means to develop a Schiff base sensor that obviates the need to compare the induced CD signals observed upon amine binding to those obtained with a reference of known absolute configuration.

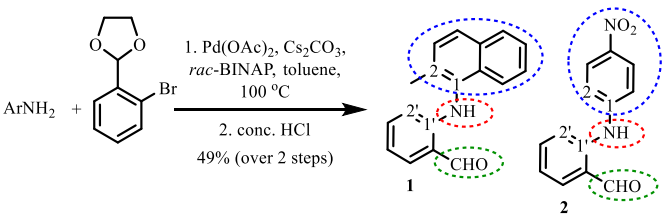

Scheme 1 Preparation and structures of sensors **1** and **2**. Blue: CD sensing chromophore. Red: proximate H-donor, Green: Amine binding site.

The readily available 2-aminobenzaldehyde scaffold carrying a hydrogen bond donating secondary diarylamine unit adjacent to the formyl group appeared to be an attractive starting point for this study because this arrangement was expected to facilitate the condensation

Department of Chemistry, Georgetown University
37th and O Streets, Washington, DC 20057 (USA)
E-mail: cw27@georgetown.edu
Department of Industrial Chemistry "Toso Montanari", University of Bologna
Viale Risorgimento 4, 40136 Bologna (ITALY)
E-mail: andrea.mazzanti@unibo.it
Homepage: http://www.thewolfgrouponline.com/
Electronic Supplementary Information (ESI) available: [details of any supplementary information available should be included here]. See DOI: 10.1039/x0xx00000x

with an amine substrate and limit the conformational freedom of the corresponding Schiff base product (Scheme 1). We considered that the 2-aminobenzaldehyde core needed to be linked to an additional UV-chromophoric group with a strong UV transition in the low-energy region of the UV spectrum. This is generally considered desirable because it reduces the possibility that CD-active impurities interfere with the chiroptical sensing event. In addition, solvents having a relatively high wavelength cut-off (e.g. chloroform) can be used. Within the obvious choice of an aromatic component as the UV-absorbing moiety, this could be either a locally C_2-symmetric or an asymmetric aryl ring. In the first case, the two conformations generated by a 180° rotation of the aryl ring around the N-C bond are homomeric, whereas in the second case two diastereoisomeric conformations are generated. Since the goal is to develop a strong CD signal induced by the chirality of the analyte, an highly unbalanced conformational equilibrium is advisable in the case of a non-C_2-symmetric sensor. In an optimal scenario, only one conformation of the sensor would be populated so that the experimental CD spectrum is not a complicate weighted average of several conformational contributions.

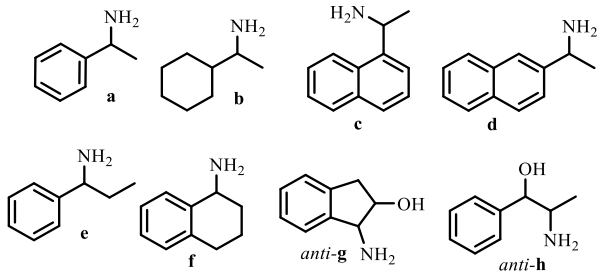

Fig. 1 Structures of selected substrates.

We envisioned that the chirality of a covalently attached amine would control the relative orientation of the chromophores in these sensor designs and thus generate characteristic Cotton effects that one could systematically correlate to the absolute configuration of the substrate. We therefore focused our attention on the two chemical structures resulting from the coupling of 2-bromobenzaldeyde with 2-methyl-1-naphthylamine (compound **1**) and *p*-nitroaniline (compound **2**). Both designs possess a strong chromophoric group in the low energy region of the UV spectrum, each with different geometric constraints and with different orientations of the UV-absorbing dipoles. The synthesis of the desired probes was accomplished via conventional coupling chemistry using commercially available aryl amines and protected bromobenzaldehyde (Scheme 1 and ESI). Subsequent deprotection of the aldehyde group was carried out under acidic conditions, producing both **1** and **2** in 49% overall yield. The test amines selected for this study are shown in Figure 1.

Results and Discussion

We first investigated the UV properties of the sensors. The geometries of **1** and **2** exhibiting an intramolecular hydrogen bond between the NH and the carbonyl moieties were optimized using B3LYP[12] and the 6-311++G(2d,p) basis set, including the solvent with the IEF-PCM formalism.[13] The UV spectra were simulated with TD-DFT at the CAM-B3LYP/6-311++G(2d,p) level.[14] The sterically demanding 2-methylnaphtyl group in **1** is skewed toward an orthogonal position to reduce steric repulsion, whereas the lack of steric hindrance at the *p*-nitrophenyl ring in sensor **2** favors a coplanar arrangement between the two aryl rings due to increased resonance stabilization.[15]

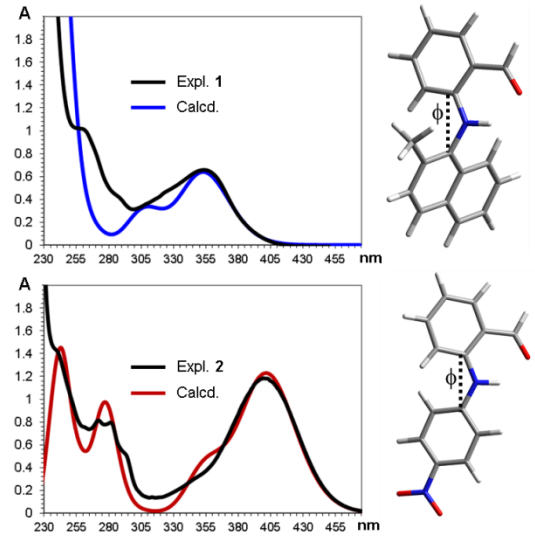

Fig. 2 Experimental and calculated UV spectra of sensors **1** and **2**. Calculations at the TD-CAM-B3LYP/6-311++G(2d,p) level. Calculated spectra were red-shifted by 25 nm (**1**) and 55 nm (**2**). The ground state geometries, where ϕ defines the dihedral angle between the two aromatic rings, are shown on the right.

As a result, the two aryl rings in **1** are almost perpendicular, with a dihedral angle ϕ of about |90|°. On the contrary, the ground state geometry of sensor **2** displays the two aromatic rings with a

significantly smaller dihedral angle of |34|° (the measured dihedral is defined by C_2-C_1-$C_{1'}$-$C_{2'}$, ϕ, as depicted in Figure 2). The two sensors have a strong UV band in the low-energy region (Figure 2). In sensor **1** the calculated band is centered at 328 nm (experimental value 363 nm), and in sensor **2** it is centered at 347 nm (experimental value 402 nm). In both cases, this band is generated by a single transition, albeit different molecular orbitals (MO) are involved (Figure 3). In the case of **1**, the main component of the UV transition is the HOMO-LUMO (81%), with the LUMO localized mainly on the aminobenzaldehyde ring whereas the HOMO is mainly present on the naphthyl ring. A minor contribution (13%) comes from the (HOMO-1)–LUMO transition. In both transitions there is a strong difference in the shapes of the MO densities and thus the UV transition of sensor **1** is suggested to be a charge transfer (CT) absorption band. In compound **2** the MO's involved in the transition are the HOMO–LUMO (81%) and the HOMO–(LUMO+1) (12%). Both transitions (particularly the HOMO-LUMO) involve two MO's that are spread over both aryl rings. Therefore, in the case of **2** the low-energy UV band is suggested to be a standard π-π* band.

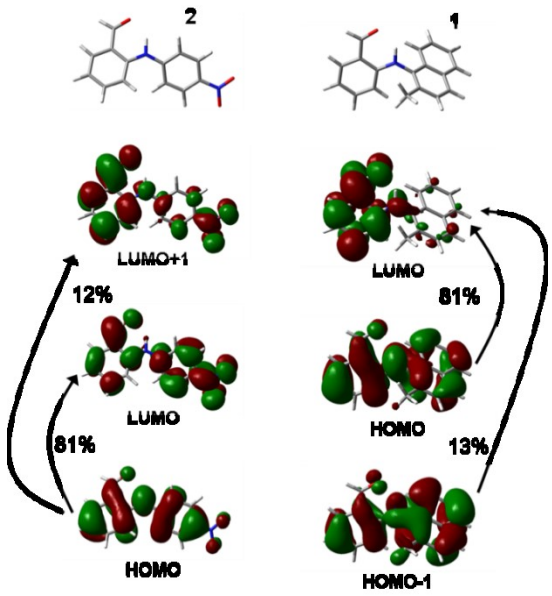

Fig. 3 MO's involved in the low energy UV absorption band of sensors **1** and **2**.

A full conformational search on compound **2a**, derived from sensor **2** and (*R*)-1-phenylethylamine, **a**, was performed using Macromodel[16] and the MMFF force field by retaining all the conformations within the 10 kcal/mol energy range. Redundant conformations were then removed (1.0 Å RMS deviation) and the remaining structures were further optimized with DFT (Gaussian 16[17]) at the B3LYP/6-31G(d) level of theory. After DFT optimization, only 4 conformations were found within a 3.0 kcal/mol limit (Figure 4). These conformations all reflect that the imino moiety is stabilized by an intramolecular hydrogen bond with the NH group intrinsic to the sensor scaffold. The four conformations differ in regards to the position of the aromatic ring of the 1-phenylethylamino moiety (**c1** *vs* **c4** and **c2** *vs* **c3**), and in the dihedral angle between the *p*-nitrophenyl ring and the 2-iminophenyl moiety (C_2-C_1-N-$C_{1'}$ in Figure 4), that can be ≈+160° (**c1** and **c4**) or –160° (**c2** and **c3**). When further optimized at the B3LYP/6-311++G(2d,p) level and including the solvent in the calculations (IEF-PCM, acetonitrile), conformations **c1** and **c2** were very close in energy, whereas **c3** and **c4** were significantly higher in energy. It should be noted that in the two most stable conformations, the CH of the stereogenic carbon is coplanar with the imino CH. Conformations that did not depict the coplanar motif were found to be much higher in energy.

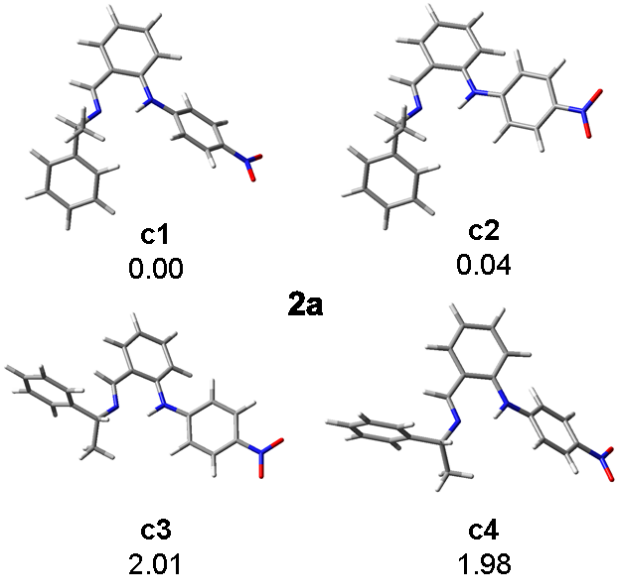

Fig. 4 The four available conformations of compound **2a**. Relative energies in kcal/mol at the PCM-B3LYP/6-311++G(2d,p) level.

The molecular mechanics (MM) conformational search performed for compound **1a** led to a similar situation, and only four conformations were found to exist within the 3 kcal/mol energy

window (Figure 5). Again, the two most stable conformations are very close in energy and possess opposite dihedral angles between the 2-methylnaphthyl ring and the 2-iminophenyl unit. As in the case of **2a**, the CH of the stereogenic carbon is coplanar with the imino CH.

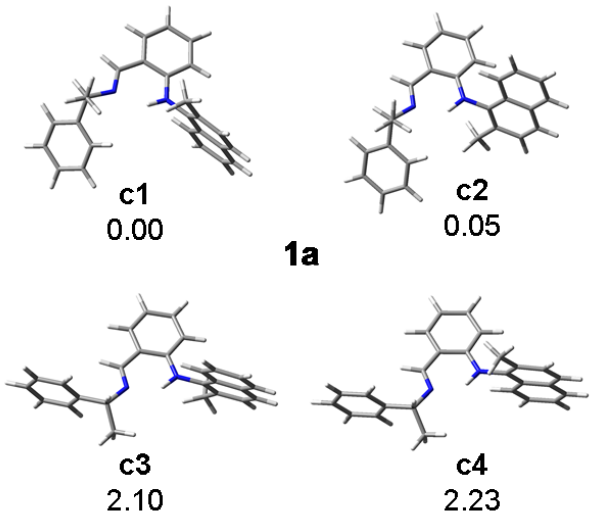

Fig. 5 Calculated conformations of **1a**. Relative energies in kcal/mol at the PCM-B3LYP/6-311++G(2d,p) level.

The CD spectra of the Schiff bases **1a** and **2a** were simulated with TD-DFT[18] starting from the geometries obtained with the larger basis set. CD simulations were obtained using the range-separated CAM-B3LYP functional and the 6-311++G(2d,p) basis set, a combination known to have good accuracy at a reasonable computational cost.[19] Because of our particular interest in the simulation of the low-energy region of the ECD spectrum, only this part of the UV/CD spectrum was simulated (see ESI for details).

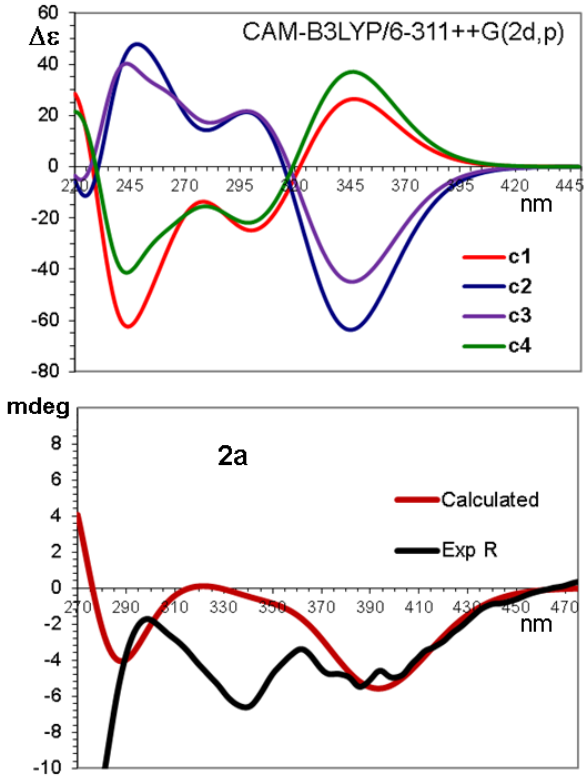

Fig. 6. Top: ECD simulations for the four conformations of compound **2a**, obtained at the TD-CAM-B3LYP/6-311++G(2d,p) level. Bottom: Simulated ECD spectrum obtained using the conformational ratio derived from the energies reported in Figure 4. The simulated spectrum was shifted by 50 nm.

The lowest energy transition for compound **2a** was calculated at ~340 nm, and it was generated mainly by the HOMO–LUMO transition, with a smaller contribution from the HOMO–(LUMO+1) transition (Figure S1 in ESI). Analysis of the MO shapes showed that only the dipoles of the sensor are involved in this CD transition and that the sign of the Cotton effect is related to the different helicity of the *p*-nitrophenyl ring with respect to the *o*-aminobenzaldehyde ring (see ESI). Accordingly, conformations **c1** and **c4**, as well as the **c2**/**c3** pair have the same CD sign.

The opposite Cotton effects of the diastereomeric species complicate the simulation of the experimental CD which is expected to be the weighted average of the individual conformational contributions. Since conformations **2a-c1** and **2a-c2** are calculated to be very close in energy, the sign of the CD transition will be determined by the effect of the enantiopure amine on the conformational balance of the two conformations. A single crystal of

the imine formed from **2** and (*S*)-1-phenylethylamine was obtained by slow evaporation of a methanol solution.[20] This solid-state structure corresponds to conformation **c2**, which is one of the two calculated to be most stable. While only this conformation is present in the solid state, both conformations are expected to be present with similar populations in solution. Nevertheless, the Boltzmann-weighted averaged ECD spectrum obtained by using the relative enthalpies[§] derived for conformations **c1**-**c4** yields a negative CD band, as experimentally observed.

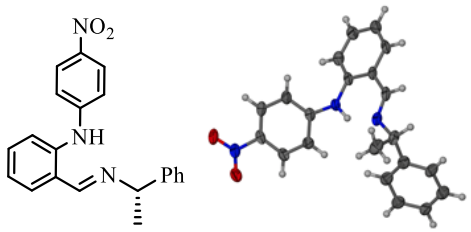

Fig 7. Single crystal structure of **2a**.

The rotational asymmetry of the 2-methylnaphtyl moiety in compound **1a** yields different results. The ECD simulations suggest that the two most stable conformations (**1a-c1** and **1a-c2**) do not have opposite signals as was the case for **2a**. The spectrum of **1a-c1** is very weak in the 290-350 nm region, whereas that of **c2** is strongly negative (when *R*-phenylethylamine **a** is used). As a result, sensor **1** seems to be more suitable because the sign of the low-energy Cotton effect should not be influenced by the conformational isomerism. The low-energy UV/CD band of **1a** mainly originates from the HOMO–LUMO and HOMO–(LUMO+1) transitions (see Figure S2 in ESI). It should be noted that the UV spectrum of compound **2a** has a maximum absorbance very close to that of the sensor alone (400 vs 396 nm, respectively, see ESI), whereas the UV spectrum of **1a** is red-shifted by approximately 22 nm with respect to that of the free sensor (376 vs 354 nm, Figure S3 in ESI). This feature can be related to the modification of the shapes of the involved MOs because the LUMO of **1a** is localized on both the aryl rings and the transition is therefore more ascribable to a classical π–π* absorption than to a charge-transfer transition which is the case with the free sensor **1**.

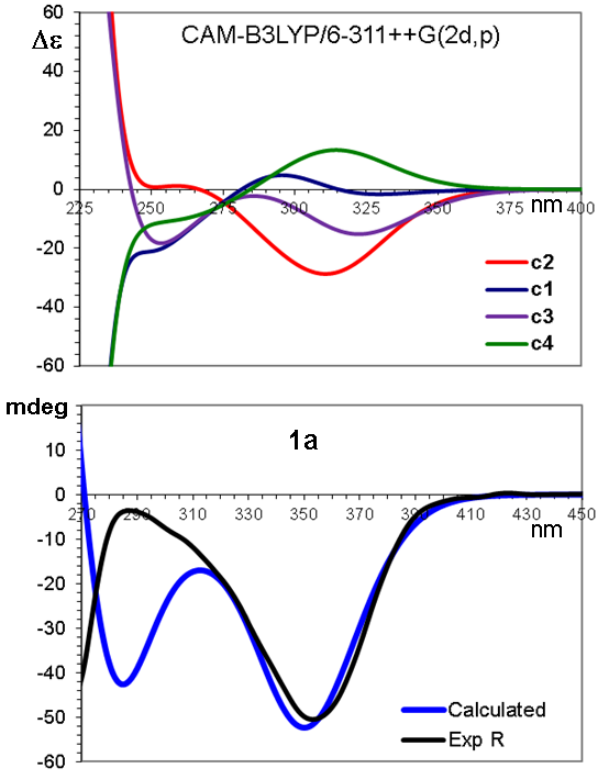

Fig 8. Top: ECD simulations for the four conformations of compound **1a**, obtained at the TD-DFT CAM-B3LYP/6-311++G(2d,p) level. Bottom: Simulated ECD spectrum obtained using the conformational ratio derived from the energies reported in Figure 5. The simulated spectrum was red-shifted by 35 nm.

To compare whether the CD spectra are affected by the presence of the aromatic ring in amine **a**, we calculated the ECD spectra of the two compounds (**1b** and **2b**) derived from (*R*)-1-cyclohexylethylamine, **b**, which is devoid of a chromophoric group. After conducting an MM conformational search and DFT optimization, four conformers were found within 3.0 kcal/mol from the global minimum (Figure S4 in ESI). In the two most prevalent conformations (**c1** and **c2**), the stereogenic carbon of the amine is in the equatorial position of the cyclohexane ring, whereas it is in the axial position in **c3**. In analogy to compounds **1a** and **2a**, the most stable conformations display the CH on the stereogenic carbon coplanar with the CH of the imino group which was also observed in the solid-state X-ray structure of **2a**. By contrast, the fourth conformation has the methyl group coplanar with the imino CH group, but its relative energy is quite high (2.96 kcal/mol). However, the two aromatic rings of the sensor moiety exhibit dihedral angles below |40|° (ϕ defined as in Figures 1). Given the inability of MMFF to

successfully manage conjugative effects, we envisioned that more conformations must be considered, because the helicity between the two aromatic rings is a key factor for the profile of the resulting ECD spectrum. Starting from conformations **c1-c4** found by the MM search, we built four new input geometries (**c1'-c4'**) with opposite dihedral angles between the two aromatic groups. As expected, the energies of conformations **c1'-c4'** were found to be very close to the corresponding conformations **c1-c4**. Simulation of the ECD spectra generated two groups of CD spectra with opposite shape due to the opposite dihedral angle between the aromatic rings of the sensor. The conformational ratio used for the simulation of the experimental spectrum was derived from optimization at the PCM-B3LYP/6-311++G(2d,p) level including the solvent acetonitrile. As for compound **2b**, the lowest energy CD band is suggested to be negative and in fair agreement with the experimental data (Figure S5 in ESI). However, the overall reliability is greatly reduced because the calculated spectrum is very sensitive to the conformational isomerism of the sensor.

When sensor **1** binds 1-cyclohexylethylamine, **1b**, the steric bulk of the 2-methylnaphthyl moiety forces the naphthyl ring to be perpendicular to the other aromatic ring. Four conformations were found through the MM search, corresponding to the two different helicities of the sensor moiety, combined with a different disposition of the cyclohexane ring, where the axial CH can be *anti* (**c2** and **c4**) or *gauche* (**c1** and **c3**) to the CH at the stereogenic carbon. The conformations in which the CH resides in the axial position of the cyclohexane ring (**c5**) or where the CH of the stereogenic carbon remains *anti* to the imine CH (**c6**) had very high energies (Figure S6 in ESI). Again, the conformation of the sensor is the only apparent factor responsible for the shape of the ECD spectrum but the number of conformations to be considered is largely reduced compared to sensor **2**. More importantly, some conformations (**c1** and **c2**) have very weak bands in the 280-350 nm region (Figure S7 in ESI, top), whereas conformations **c3** and **c4** have negative bands in the same region. Thus, the Boltzmann-averaged spectrum in the UV region of interest is almost insensitive to the employed conformational ratio (Figure S5 in ESI, bottom). Altogether, we conclude that sensor **1** greatly simplifies the determination of the absolute configuration of chiral amines and the sense of chirality induction based on the steric considerations discussed above is expected to be of general value.

With this analysis in hand, we then tested the utility of both probes for the sensing of amines **c-h**. The condensations were carried out using either dichloromethane or acetonitrile as solvent and the reaction mixtures were then diluted with acetonitrile and subjected to CD analysis without further purification. In all cases, the imine formation proceeds smoothly at room temperature in the presence of molecular sieves and we observed positive Cotton effects at micromolar concentrations upon binding of the (*S*)-amines while the Schiff base formation with the (*R*)-enantiomers gave the opposite chiroptical signal (see ESI). Representative examples are shown in Figure 9.

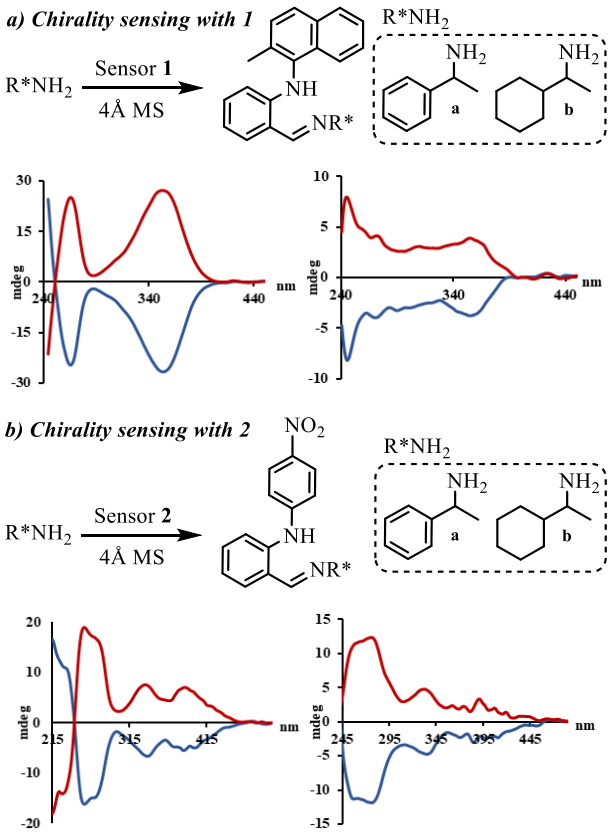

Fig 9. Representative examples of chiroptical amine sensing. a) CD signals of the imines obtained using **1** and (*R*)-1-phenylethylamine (blue) or (*S*)-1-phenylethylamine (red) at 68 μM in ACN (left), **1** and (*R*)-1-cyclohexylethylamine (blue) or (*S*)-1-cyclohexylethylamine (red) at 68 μM (right). b) CD results using **2** for (*R*)-1-phenylethylamine (blue) and (*S*)-1-phenylethylamine (red) at 60 μM (left), and with (*R*)-1-cyclohexylethylamine (blue) or (*S*)-1-cyclohexylethylamine (red) at 90 μM (right).

Finally, we decided to explore the possibility of quantitative *ee* analysis of amine **e** with sensor **1**. Using essentially the same sensing

protocol, we first determined a calibration curve of the CD maximum of the imine product measured at 354 nm versus the sample *ee* values (Figure 10). This was then used to determine the enantiomeric composition of four nonracemic samples. Our sensing analysis revealed the correct absolute configuration of the major enantiomer based on the sign of the observed Cotton effect. Additionally, it allowed for the determination of the sample *ee* values with sufficient accuracy for high-throughput screening purposes (Table 1 and ESI). For example, the CD sensing of the samples containing the (*S*)-amine in 87 and 76% *ee* gave 93 and 74% *ee*, respectively (entries 1 and 2).

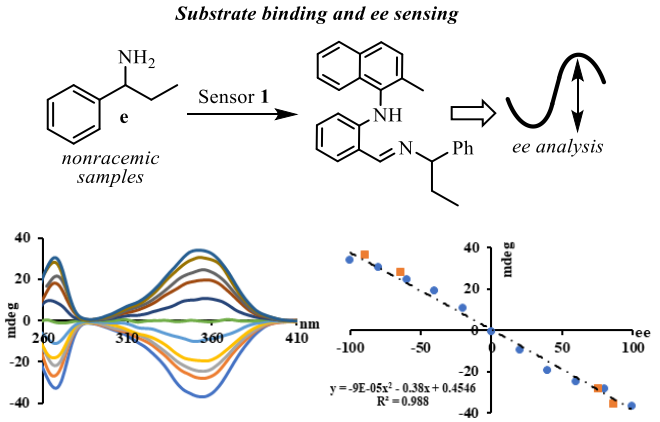

Fig 10. Quantitative *ee* analysis using sensor **1**. Calibration curve of the chiroptical responses of **1** with varied enantiomeric compositions of 1-phenylpropan-1-amine (left) and polynomial fitting of the sensor-tethered analyte CD responses at 354 nm versus the *ee* values of each scalemic sample (blue). The CD results with random *ee* compositions of **e** are shown in orange.

Table 1. CD Sensing of nonracemic samples of amine **e** using sensor **1**.

Sample composition		Chiroptical sensing results	
absolute configuration	*ee* values (%)	absolute configuration	*ee* values (%)
S	87	*S*	93
S	76	*S*	74
R	64	*R*	73
R	89	*R*	97

Conclusions

In summary, we have prepared and tested chiroptical sensors exhibiting a 2-aminobenzaldehyde derived scaffold with a hydrogen bond donating secondary diarylamine unit adjacent to the formyl group which allows Schiff base formation with amines. The covalent binding of a chiral amine substrate affects the conformational bias in the sensor moiety which results in characteristic CD spectra. Computational analysis revealed that CD prediction and thus determination of the absolute configuration of the substrate becomes practical with a sterically crowded sensor design as the number of conformations to be considered is largely reduced while the induced CD spectrum is less sensitive to conformational equilibria. Finally, the possibility of quantitative *ee* analysis of nonracemic amine samples was demonstrated.

Conflicts of interest

There are no conflicts to declare.

Acknowledgements

S.L.P. and C.W. are grateful for financial support from the U.S. National Science Foundation (CHE-1764135). A.M. and M.M. thank the University of Bologna (RFO funds 2017 and 2018).

Notes and references

§ In the entirety of the manuscript we decided to use the ZPE-corrected enthalpies instead of the Gibbs free energy because of the presence of many low-value vibrational normal modes that hamper a correct evaluation of the entropic factor. See ESI for details and references.

1 L. Pu,. *Chem. Rev.* 2004, **104**, 1687; D. Leung, S. O. Kang, and E. V. Anslyn, *Chem. Soc. Rev.* 2012, **41**, 448; C. Wolf, and K. W. Bentley, *Chem. Soc. Rev.* 2013, **42**, 5408; B. T. Herrera, S. L. Pilicer, E. V. Anslyn, L. A. Joyce, and C. Wolf, *J Am. Chem. Soc.* 2018, **140**, 10385.

2 X. Huang, B. H. Rickman, B. Borhan, N. Berova, and K. Nakanishi, *J. Am. Chem. Soc.,* 1998**, 120**, 6185; X. Huang, B. Borhan, B. H. Rickman, K. Nakanishi, and N. Berova, *Chem. - Eur. J.,* 2000, **6**, 216.; X. Huang, N. Fujioka, G. Pescitelli, F. E. Koehn, R. T. Williamson, K. Nakanishi, and N. Berova, *J. Am. Chem. Soc.* 2002, **124**, 10320; N. Berova, G. Pescitelli, A. G. Petrovic, and G. Proni, *Chem. Commun.* 2009, 5958.

3 H. Kim, S. M. So, C. P.-H. Yen, E. Vinhato, A. J. Lough, J.-I. Hong, H.-J. Kim, and J. Chin, *Angew. Chem. Int. Ed.* 2008, **47**, 8657; Seo, M.-S., Lee, A., Kim, H., *Org. Lett.* 2014, **16**, 2950.

4 J. F. Folmer-Andersen, V. M. Lynch, and E. V. Anslyn, *J. Am. Chem. Soc.* 2005, **127**, 7986; S. Nieto, V. M. Lynch, E. V. Anslyn, H. Kim, and J. Chin, *J. Am. Chem. Soc.* 2008*,* **130**, 9232; D. Leung, and E. V. Anslyn, *J. Am. Chem. Soc.* 2008, **130**, 12328.; S. Nieto, V. M. Lynch, E. V. Anslyn, H. Kim, J. Chin, *Org. Lett.* 2008, **10**, 5167; S. Nieto, J. M. Dragna, and E. V. Anslyn, *Chem. Eur. J.* 2010, **16**, 227; J. M. Dragna, G. Pescitelli, L. Tran, V. M. Lynch, E. V. Anslyn, and L. Di Bari, *J. Am. Chem. Soc.* 2012, **134**, 4398; P. Metola, E. V. Anslyn, T. D. James, and S. D. Bull, *Chem. Sci.,* 2012, **3**, 156; J. M. Dragna, A. M. Gade, L. Tran, V. M. Lynch, V. M., and E. V. Anslyn, *Chirality,* 2015, **27**, 294; C. Ni, D. Zha, H. Ye, Y. Hai, Y. Zhou, E. V. Anslyn, and L. You, *Angew. Chem. Int. Ed.* 2018, **57**, 1300.

5 E. G. Shcherbakova, T. Minami, V. Brega, T. D. James, and P. Anzenbacher, Jr., *Angew. Chem. Int. Ed.* 2015, **54**, 7130; E. G. Shcherbakova, V. Brega, T. Minami, S. Sheykhi, T. D. James, and P. Anzenbacher, Jr, *Chem. Eur. J.,* 2016, **22**, 10074; M. Pushina, S. Farshbaf, E. G. Shcherbakova, and P. Anzenbacher, *Chem. Commun.* 2019, **55**, 4495.

6 V. J. Pugh, Q. S. Hu, X. Zuo, F. D. Lewis, and L. Pu, *J. Org. Chem.* 2001, **66**, 6136; Q. Wang, X. Chen, L. Tao, L. Wang, D. Xiao, X. Q. Yu, and L. Pu, *J. Org. Chem.,* 2007, **72**, 97; S. Yu, W. Plunkett, M. Kim, and L. Pu, *J. Am. Chem. Soc.* 2012, **134**, 20282; Z. Huang, S. Wu, X. Zhao, K. Wen, Y. Xu, X. Yu, Y. Xu, and L. Pu, *Chem. Eur. J.* 2014, **20**, 16458; K. Wen, S. Yu, Z. Huang, L. Chen, M. Xiao, X. Yu, and L. Pu, *J. Am. Chem. Soc.* 2015, **137**, 4517; C. Wang, E. Wu, X. Wu, X. Xu, G. Zhang, and L. Pu, *J. Am. Chem. Soc.* 2015, **137**, 3747; L. Hu, S. Yu, Y. Wang, X. Yu, and L. Pu, *Org. Lett.* 2017, **19**, 3779; H. L. Liu, H. P. Zhu, X. L. Hou, and L. Pu, *Org. Lett.* 2010, **12**, 4172.

7 M. Anyika, H. Gholami, K. D. Ashtekar, R. Acho, and B. Borhan, *J. Am. Chem. Soc.* 2014, **136**, 550; J. Zhang, H. Gholami, X. Ding, M. Chun, C. Vasileiou, T. Nehira, and B. Borhan, *Org. Lett.* 2017, **19**, 1362.

8 R. Peng, L. Lin, X. Wu, X. Liu, X. Feng, *J. Org. Chem.* 2013, **78**, 11602. X. Wu, M. Xie, X., Zhao, X. Liu, L. Lin, X. Feng, *Tetrahedron Lett.* 2014, **55**, 3446. X. He, Q. Zhang, X. Liu, L. Lin, X. Feng, *Chem. Commun.* 2011, **47**, 11641.

9 X. Mei, and C. Wolf, C., *J. Am. Chem. Soc.* 2006, **128**, 13326; M. W. Ghosn, and C. Wolf, *J. Am. Chem. Soc.* 2009, **131**, 16360; M. W. Ghosn, and C. Wolf, *Tetrahedron* 2010, **66**, 3989; D. P. Iwaniuk, and C. Wolf, *J. Am. Chem. Soc.* 2011, **133**, 2414; M. W. Ghosn, C. Wolf, C., *J. Org. Chem.* 2011, **76**, 3888; D. P. Iwaniuk, and C. Wolf, *Org. Lett.* 2011, **13**, 2602; D. P. Iwaniuk, K. W. Bentley, and C. Wolf, *Chirality,* 2012, **24**, 584; K. W. Bentley, and C. Wolf, *J. Am. Chem. Soc.* 2013, **135**, 12200. K. W. Bentley, Y. G. Nam, J M. Murphy, and C. Wolf, *J. Am. Chem. Soc.* 2013, **135**, 18052. K. W. Bentley, and C. Wolf, *J. Org. Chem.* 2014, **79**, 6517; Z. A. De los Santos, R. Ding, and C. Wolf, *Org. Biomol. Chem.* 2016, **14**, 1934; Z. A. De los Santos, and C. Wolf, *J. Am. Chem. Soc.* 2016, **138**, 13517; S. L. Pilicer, P. R. Bakhshi, K. W. Bentley, and C. Wolf, *J. Am. Chem. Soc.,* 2017, **139**, 1758; F. Y. Thanzeel, K. Balaraman, and C. Wolf, *Nat. Comm.* 2018, **9**, 5323; F. Y. Thanzeel, and C. Wolf, *Angew. Chem. Int. Ed.,* 2017, **56**, 7276.

10 J. Zhang, A. E. Holmes, A. Sharma, N. R. Brooks, R. S. Rarig, J. Zubieta, and J. W. Canary, *Chirality,* 2003, **15**, 180; J. Sciebura, and J. Gawronski, *Chem. Eur. J.* 2011, **17**, 13138; L. A. Joyce, E. C. Sherer, and C. J. Welch, *Chem. Sci.* 2014, **5**, 2855; P. Zardi, K. Wurst, G. Licini, and C. Zonta, *J. Am. Chem. Soc.* 2017, **139**, 15616; For a noncovalent binding approach: F. Biedermann, and W. M. Nau, *Angew. Chem. Int. Ed.* 2014, **53**, 5694; S. Vergura, P. Scafato, S. Belviso, and S. Superchi, *Chem. Eur. J.* 2019, **25**, 5682.

11 P. Metola, S. M. Nichols, B. Kahr, and E. V Anslyn, *Chem. Sci.* 2014, **5**, 4278.

12 C. Lee, W. Yang, R. G. Parr, *Phys. Rev. B.* 1988, **37**, 785; A. D. Becke, *J. Chem. Phys.* 1993, **98**, 5648; P. J. Stephens, F. J. Devlin, C. F. Chabalowski, and J. M. Frisch, *J. Phys. Chem.* 1994, **98**, 11623.

13 J. Tomasi, B. Mennucci, and R. Cammi, *Chem. Rev.* 2005, **105**, 2999.

14 T. Yanai, D. Tewand, D., and N. Handy, *Chem. Phys. Lett.* 2004, **393**, 51.

15 L. Lunazzi, A. Mazzanti, M. Minzoni, and J. E. Anderson, *J. Org. Chem.* 2006, **71**, 5474.

16 Schrödinger Release 2019-1: MacroModel, Schrödinger, LLC, New York, NY, 2019.

17 Gaussian 16, Revision A.03, M. J. Frisch, G. W. Trucks, H. B. Schlegel, G. E. Scuseria, M. A. Robb, J. R. Cheeseman, G. Scalmani, V. Barone, G. A. Petersson, H. Nakatsuji, X. Li, M. Caricato, A. V. Marenich, J. Bloino, B. G. Janesko, R. Gomperts, B. Mennucci, H. P. Hratchian, J. V. Ortiz, A. F. Izmaylov, J. L. Sonnenberg, D. Williams-Young, F. Ding, F. Lipparini, F. Egidi, J. Goings, B. Peng, A. Petrone, T. Henderson, D. Ranasinghe, V. G. Zakrzewski, J. Gao, N. Rega, G. Zheng, W. Liang, M. Hada, M. Ehara, K. Toyota, R. Fukuda, J. Hasegawa, M. Ishida, T. Nakajima, Y. Honda, O. Kitao, H. Nakai, T. Vreven, K. Throssell, J. A. Montgomery, Jr., J. E. Peralta, F. Ogliaro, M. J. Bearpark, J. J. Heyd, E. N. Brothers, K. N. Kudin, V. N. Staroverov, T. A. Keith, R. Kobayashi, J. Normand, K. Raghavachari, A. P. Rendell, J. C. Burant, S. S. Iyengar, J. Tomasi, M. Cossi, J. M. Millam, M. Klene, C. Adamo, R. Cammi, J. W. Ochterski, R. L. Martin, K. Morokuma, O. Farkas, J. B. Foresman, and D. J. Fox, Gaussian, Inc., Wallingford CT, **2016**.

18 S. Superchi, P. Scafato, M. Górecki, and G. Pescitelli. *Curr. Med. Chem.* **2018**, *25*, 287. See also: a) M. Srebro-Hooper, and J. Autschbach, *Annu. Rev. Phys. Chem.* **2017**, *68*, 399. b) G. Pescitelli, and T. Bruhn. *Chirality*, **2016**, *28*, 466.

19 M. Meazza, M. Kamlar, L. Jašíková, B. Formánek, A. Mazzanti, J. Roithová, J. Veselý, and R. Rios, *Chem. Sci.*, **2018**, *9*, 6368; G. Di Carmine, D. Ragno, O. Bortolini, P. P. Giovannini, A. Mazzanti, A. Massi, and M. Fogagnolo. *J. Org. Chem.* **2018**, *83,* 2050; M. Mancinelli, S. Perticarari, L. Prati, and A. Mazzanti, *J. Org. Chem.* **2017**, *82*, 6874; M. Meazza, M. E. Light, A. Mazzanti, and R. Rios, *Chem. Sci.* **2016**, *7*, 984; P. Gunasekaran, S. Perumal, J. Carlos Menéndez, M. Mancinelli, S. Ranieri, and A. Mazzanti, *J. Org. Chem.* **2014**, *79,* 11039.

20 The CCDC number 1896570 contains the supplementary crystallographic data for this paper. These data can be obtained free of charge from the Cambridge Crystallographic Data Centre.